Supporting Information

Fast Switching of Spontaneous Polarization in a Microporous Molecular Rotor Ferroelectric

Le-Ping Miao[a†], Ning Ding[b†], Na Wang[a], Heng-Yun Ye[a], Chao Shi[a*] and Shuai Dong[b*]

a Chaotic Matter Science Research Center, Jiangxi Provincial Key Laboratory of Functional Molecular Materials Chemistry, Jiangxi University of Science and Technology, Ganzhou 341000, China.

b School of Physics, Southeast University, Nanjing 211189, China.

† These authors contributed equally: Le-Ping Miao, Ning Ding.

* Correspondence and requests for materials should be addressed to C.S. or S.D. (email: 15150517670@163.com or sdong@seu.edu.cn).

Table of contents

situations (a) the NO_3^- guests are fixed and the $[CdL_4]^{2+}$ hosts are twisted gradually. (b) The $[CdL_4]^{2+}$ hosts are fixed and the NO_3^- guests are rotated gradually. Inert: the schematic of normalized "1" state.

Table S1. Crystal data for cadmium coordination compounds of amino acids.

Table S2. The lattice constants of paraelectric phase (PE) and ferroelectric phase (FE) from DFT calculation and experiments (Exp).

Reference

Experimental

Synthesis and methods

Synthesis and Crystal growth. 1 was obtained as colorless block crystals with sized up to 4×3.5×1.5 cm^3 (Figure S1) by slow evaporation of stoichiometric amounts of $Cd(NO_3)_2 \cdot 4H_2O$ and *β*-alanine. The purity of the bulk phase was verified by the powder X-ray diffraction measurement (Figure S2).

Crystal structure determination. Variable-temperature single-crystal diffraction data were collected on a Rigaku synergy diffractometer using Mo-K_α (λ= 0.71073 Å) radiation from a graphite monochromator. The crystal structures were resolved by direct method and then refined by full-matrix least-square method based on F^2 using the SHELXTL-2014 program[1]. Non-hydrogen atoms were refined anisotropically and located in difference Fourier maps, however, the positions of hydrogen atoms were generated geometrically with U_{iso} = 1.2 U_{eq} (C and N).

The detail method of the directions of the crystal **1** is that: The monocrystalline samples oriented on the Rigaku synergy diffractometer (Operating system: CrysAlisPro 1.171.41.112a (Rigaku OD, 2021)), the specific operation is as follows: We first performed the pre-experimental to confirm the unit cell parameters. Second, we clicked the axial photographic, then chose the c axial ((001) plane) and made the plane of the monocrystalline sample showed front.

Ferroelectric phase transition Measurements. Powder X-ray diffraction (PXRD) data was obtained on a Rigaku D/MAX 2000 PC X-ray diffractometer. Differential scanning calorimetry (DSC) measurements were carried out on a netzsch polyma differential scanning calorimeter under nitrogen at atmospheric pressure, with a heating/cooling rate of 10 K/min. For dielectric measurements, both the polycrystalline samples and single-crystal samples with well-defined directions were used as the plates with thickness of around 0.5 mm and area of around 10 mm^2. Silver conducting paste deposited on the plate surfaces was used as electrodes. A Tonghui TH2828A impedance analyzer was used to measure the dielectric constants. For second harmonic generation (SHG) measurements, an unexpanded laser beam with low divergence (pulsed Nd:YAG at a wavelength of 1064 nm, 5 ns pulse duration, 1.6 MW peak power, 10 Hz repetition rate) was applied. The system is based on the theory of KURTZ about the second harmonic generation of crystalline powders. SHG performance of sample was determined by comparison of the signal intensity with that of KDP (KH_2PO_4). The size of measured samples is about 200 mesh. And a Radiant Precision Premier II instrument was used to measure the *P–E* hysteresis loops and fatigue. Ferroelectric switching measurements were directly carried out on the thin film by scanning probe microscopy

technique through a resonant-enhanced PFM [MFP-3D, Asylum Research, and conductive Pt/Ir-coated silicon probes (EFM-50, Nanoworld)].

DFT Calculation. The first-principles calculations based on density functional theory (DFT) were performed with the projector augmented wave pseudopotentials as implemented in Vienna *ab initio* simulation package (VASP)[2]. The generalized gradient approximation (GGA) parametrized by Perdew, Burke, and Ernzerhof (PBE) was adopted for the exchange correlation[3]. The plane-wave cutoff energy was 550 eV. The Monkhorst-Pack k-point mesh of $1 \times 1 \times 2$ was adopted for both structural relaxation and static computation. The vdW correction of DFT-D2 method is adopted[4], which leads to the lattice constants close to the experimental value (Table S2). The convergent criterion for the energy was set to 10^{-6} eV, and that of the Hellman-Feynman force during the structural relaxation was 0.01 eV/Å. In addition, the polarization was estimated by the Berry Phase method[5,6] and the energy barriers were investigated using the nudged elastic band (NEB) method[7].

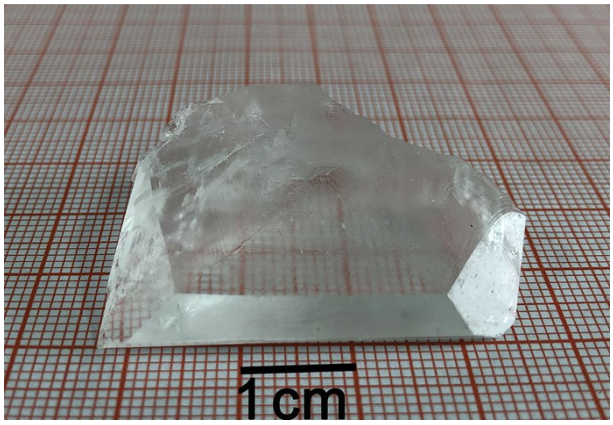

Figure S1. The macroscopic shape of the large single crystal of crystal **1**.

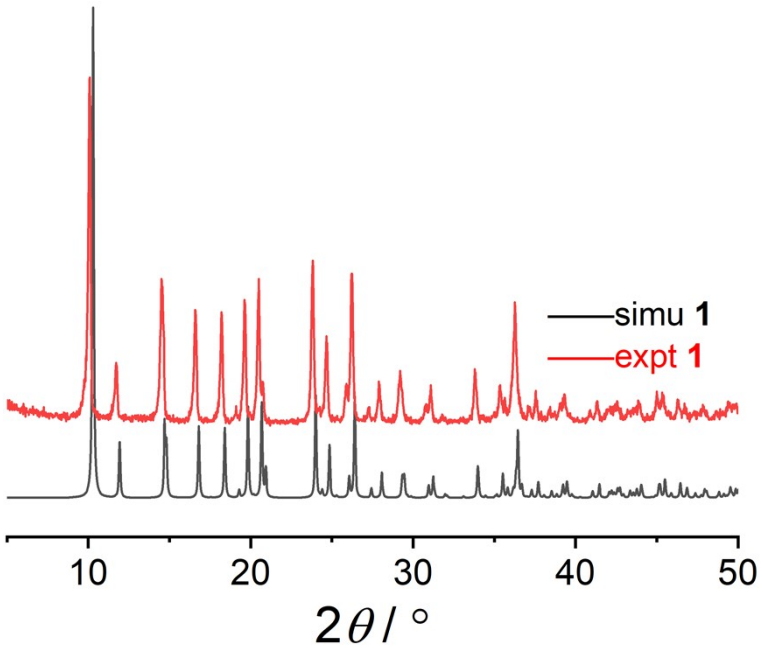

Figure S2. PXRD patterns of crystal **1**.

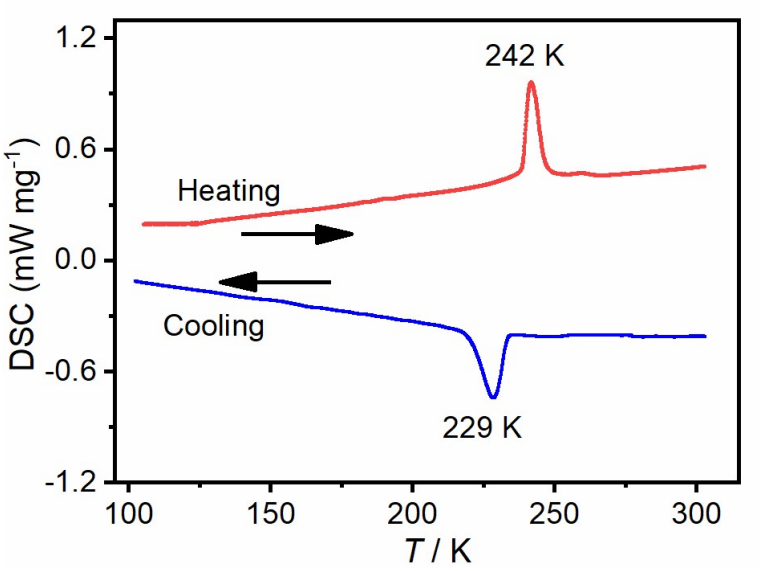

Figure S3. The DSC curves of crystal **1**.

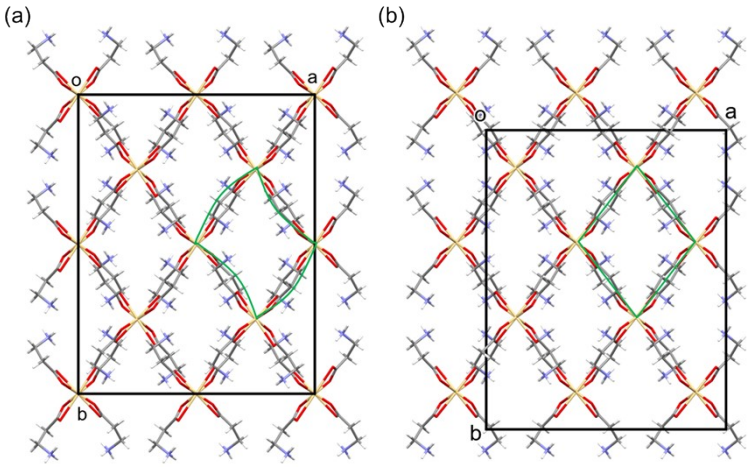

Figure S4. The twist of cationic host frameworks of **1** (a) LTP, (b) HTP.

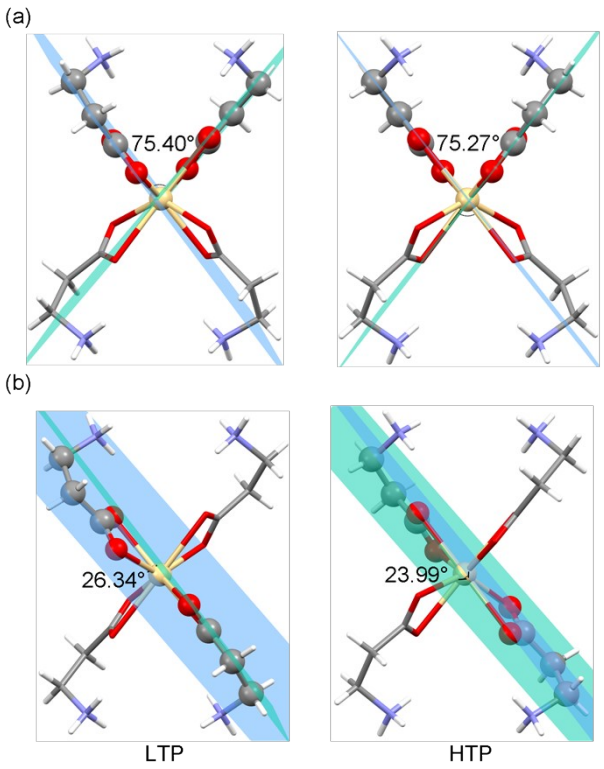

Figure S5. The changes of the dihedral angles of anionic guests of **1**.

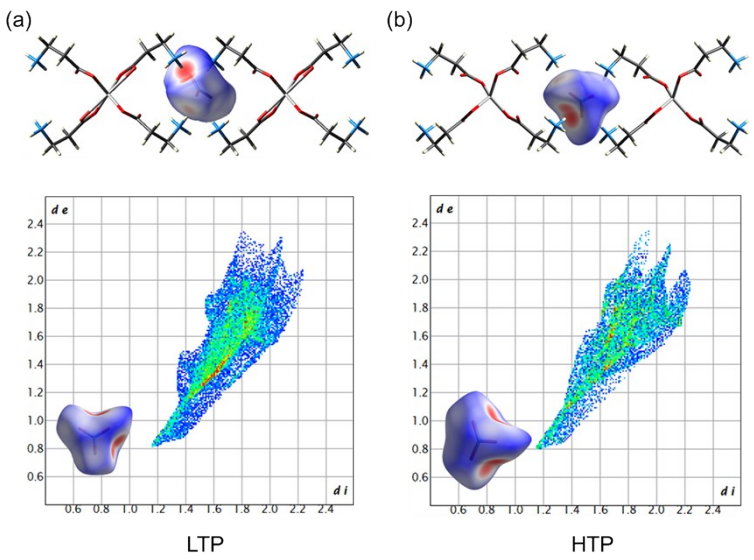

Figure S6. The visualization map of the distribution of the interactions and the 2D fingerprint plots of anionic guests of **1** (a) LTP, (b) HTP.

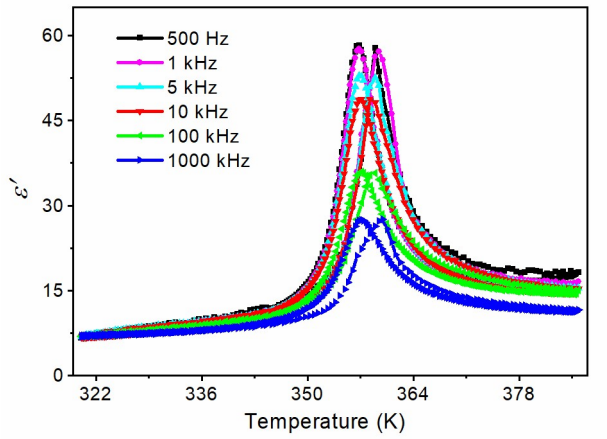

Figure S7. The curves of ε'–T, measured on powder sample of **1**.

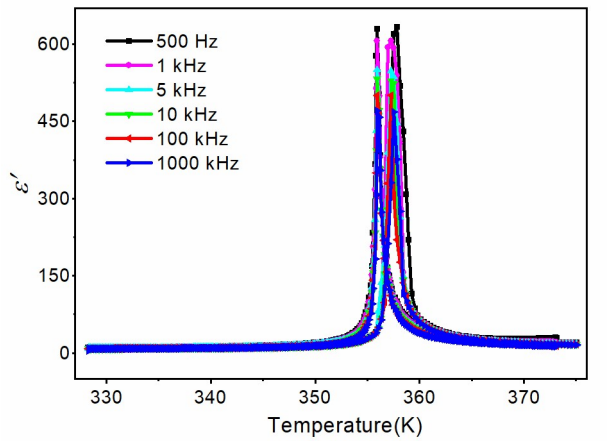

Figure S8. Dielectric response of **1** along the polar *c*-axis at various frequencies. Almost no

dispersion is observed.

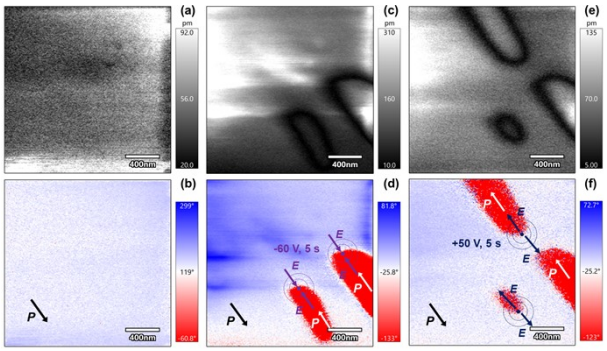

Figure S9. Detail PFM signal of amplitude and phase images are captured from the pristine domain in Figure 4 in main text.

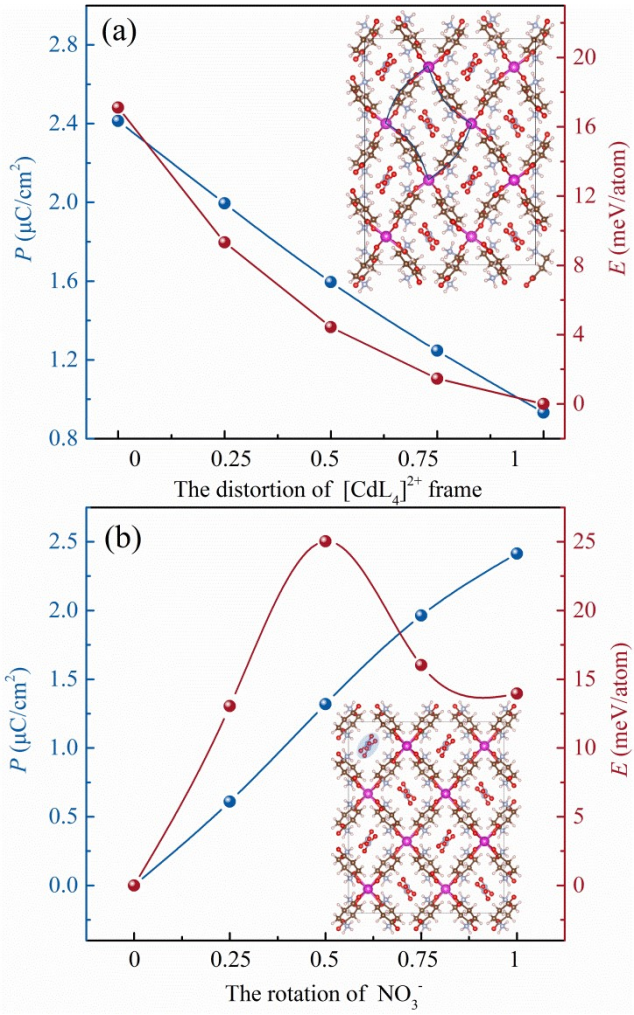

Figure S10. The polarization and energy barrier with the normalized distortion in two different situations (a) the NO_3^- guests are fixed and the $[CdL_4]^{2+}$ hosts are twisted gradually. (b) The $[CdL_4]^{2+}$

hosts are fixed and the NO_3^- guests are rotated gradually. Inert: the schematic of normalized "1" state.

Table S1. Crystal data for cadmium coordination compounds of amino acids.

1	**293 K**	**373 K**
formula	$C_{12}H_{28}N_6O_{14}Cd$	$C_{12}H_{28}N_6O_{14}Cd$
M_w	592.81	592.81
CCDC	1918863	1918864
Crystal system	Orthorhombic	Orthorhombic
space group	*Fdd2*	*Fddd*
a [Å]	18.8987(5)	19.1677(6)
b [Å]	23.8891(5)	23.9606(6)
c [Å]	10.5306(2)	10.4840(2)
α [º]	90	90
β [º]	90	90
γ [º]	90	90
V [Å^3]	4756.27(18)	4815.0(2)
Z	8	8
ρ_{calcd} [g cm^{-3}]	1.656	1.636
μ [mm^{-1}]	0.994	0.982
total reflns	6830	7840
obsd reflns ($I > 2\sigma(I)$)	2908	1713
R_{int}	0.0107	0.0111
R_1[a], wR_2[b] ($I > 2\sigma(I)$)	0.0199, 0.0543	0.0303, 0.0923
R_1[a], wR_2[b] (all data)	0.0213, 0.0549	0.0323, 0.0937
GOF (F^2)	1.070	1.097
$\Delta\rho$[c] [e Å^{-3}]	0.198, −0.353	0.477, −0.891

[a]$R_1=\Sigma||F_o|-|F_c||/|F_o|$. [b]$wR_2=[\Sigma w(F_o^2-F_c^2)^2]/\Sigma w(F_o^2)^2]^{1/2}$. [c]Maximum and minimum residual electron density.

Table S2. The lattice constants of paraelectric phase (PE) and ferroelectric phase (FE) from DFT calculation and experiments (Exp).

	a (Å)	*b* (Å)	*c* (Å)
PE (DFT)	18.948	23.289	10.011
PE (Exp)	19.167	23.961	10.484
FE (DFT)	17.869	23.704	9.902

FE (Exp)	18.899	23.899	10.531

Reference

1 G. M. Sheldrick, SHELXT-Integrated space-group and crystal-structure determination. *Acta Crystallogr*, 2015, **71**, 3–8.

2 G. Kresse, J. Furthmüller, Efficient iterative schemes for ab initio total-energy calculations using a plane-wave basis set. *Phys*. *Rev*. *B*, 1996, **54**, 11169−11186.

3 J. P. Perdew, K. Burke, B. Ernzerhof, Generalized gradient approximation made simple. *Phys*. *Rev*. *Lett*., 1996, **77**, 3865−3868.

4 S. Grimme, Semiempirical GGA-type density functional constructed with a long-range dispersion correction. *J*. *Comput*. *Chem*., 2006, **27**, 1787−1799.

5 R. D. King-Smith, D. Vanderbilt, Theory of polarization of crystalline solids. *Phys*. *Rev*. *B*, 1993, **47**, 1651−1654.

6 R. Resta, Macroscopic polarization in crystalline dielectrics: the geometric phase approach. *Rev*. *Mod*. *Phys*., 1994, **66**, 899−915.

7 G. Henkelman, B. P. Uberuaga, J. Hannes, A climbing image nudged elastic band method for finding saddle points and minimum energy paths. *J. Chem. Phys.*, 2000, **113**, 9901−9904.